

R. E. Russo, X. L. Mao, O. V. Borisov and Haichen Liu

Lawrence Berkeley National Laboratory, Berkeley, CA, 94720, USA

Received 30th May 2000, Accepted 10th June 2000

Published on the Web 9th August 2000

As laser ablation becomes more ubiquitous for direct solid sampling with inductively coupled plasma mass spectrometry (ICP-MS), the need to understand and mitigate fractionation (non-stoichiometric generation of vapor species) becomes critical. The influence of laser-beam wavelength on fractionation is not well established; in general, it is believed that fractionation is reduced as the wavelength becomes shorter. This manuscript presents an investigation of fractionation during ablation of NIST glasses and calcite using three UV wavelengths (157 nm, 213 nm and 266 nm). Fractionation can be observed for all wavelengths, depending in each case on the laser-beam irradiance and the number of laser pulses at each sample-surface location. The transparency of the sample influences the amount of sample ablated (removed) at each wavelength, and the extent of fractionation. Pb/Ca and Pb/U ratios are used as examples to demonstrate the degree of fractionation at the different wavelengths.

Introduction

Laser ablation is a viable technology for direct solid sampling into an inductively coupled plasma (ICP), with detection by atomic emission spectroscopy (AES) or mass spectrometry (MS).^{1–4} The advantages of laser ablation have clearly been established and include the ability to sample any material, minimal sample quantity (μg – ng), with little or no sample preparation. Like all analytical technologies, laser ablation requires standards for quantitative chemical analysis. If matrix-matched standards are available, laser ablation can provide accurate quantitative analysis even if fractionation occurs (in both the known standards and the unknown sample). If matrix-matched standards are not available, accuracy depends on the degree of fractionation between the sample and the standards.

It is important to put laser ablation into perspective with regard to the conventional sampling approach, liquid nebulization. Even with this established method, excellent standards (a solution with the appropriate elements and concentrations) must be prepared. For laser ablation, it may be possible to develop standards or use National Institute of Standards & Technology (NIST) materials. In these cases, calibration curves can be established and unknown samples accurately analyzed. However, for many environmental samples, standards cannot be prepared. In these cases for which matrix-matched standards do not exist, it is necessary to ensure that the ablation produces stoichiometric vapor.

The ablated mass quantity and composition are influenced by all the laser-beam properties.⁵ For stoichiometric sampling, the laser-sample interaction should be ablative (photophysical) with minimal sample heating. Such conditions can usually be achieved at higher irradiances, although the laser-induced surface plasma can contribute to radiative heating of the sample. Ablation mechanisms are influenced by the photon energy of the laser. Shorter wavelengths offer higher photon energies for bond breaking and ionization processes. The photon energy is 4.66, 5.83 and 7.90 eV for wavelengths 266, 213 and 157 nm, respectively. The lower optical penetration depth for most materials in the UV also provides more laser energy per unit volume for ablation.

The influence of laser-beam wavelength on fractionation has been addressed by the analytical community. Various wave-

lengths from nanosecond-pulsed Nd:YAG lasers have been the most commonly studied.⁶ Pb/U fractionation from NIST 610 Glass was found to be similar using 213 and 266 nm Nd:YAG lasers.⁷ Fractionation was influenced by the laser irradiance and the formation of a crater. Fractionation from NIST 610 Glass was also observed using the Nd:YAG 1064 and 266 nm wavelengths.⁸ A relationship between fractionation and ionic radius, charge and melting temperature of the elements was proposed.^{9,10} Fractionation appeared to correlate with the geochemical classification of elements; lithophiles, siderophiles, and chalcophiles when using the 266 nm Nd:YAG to ablate geological samples.¹¹ The fifth harmonic of a Nd:YAG laser (213 nm) was found to improve the ablation of strongly cleaved mineral (calcite, garnet) thin sections.¹² The 213 nm wavelength led to a more stable and higher intensity signal than that for the 266 nm laser. Fractionation of Pb and Bi from NIST 612 Glass was reduced using the 213 nm laser.

The ablation behaviour from surrogate waste-glass samples was investigated using a 100 ps pulsed Nd:YAG laser at 1064, 532 and 266 nm.¹³ The 1064 and 532 nm lasers produced elemental fractionation related to the melting point of the corresponding elemental oxide. With 266 nm, fractionation existed but was independent of the elemental oxide melting point.

Fractionation during repetitive ablation on glass samples became significant¹⁴ when the depth/diameter ratio of the ablation crater was >6 .¹⁵ Similar degrees of elemental fractionation were obtained when ablating deep craters with both 266 nm Nd:YAG and KrF 248 nm excimer lasers. Time-profiles, representing the crater etch rate or mass ablation rate, were more stable and flatter using ArF 193 nm compared to Nd:YAG 266 nm. Time-dependent elemental fractionation was found to be insignificant with the 193 nm excimer laser, whereas the Nd:YAG 266 nm laser produced significant time-dependent fractionation.¹⁶ It was not established whether the advantages of 193 nm were related to higher photoenergy or due to different beam homogenization, optics and focusing conditions.

An ArF excimer laser (193 nm) was used to ablate NIST 612 Glass samples.^{17,18} Even at this low UV wavelength, volatile-element enrichment was observed in the ICP-MS. Fractionation was found to be insignificant if a carefully selected combination of intermediate energy density ($8.5\text{--}14\text{ J cm}^{-2}$) and relatively low repetition rate ($<20\text{ Hz}$) were used. The amount of ablated

†Presented at the 2000 Winter Conference on Plasma Spectrochemistry, Fort Lauderdale, FL, USA, January 10–15, 2000.

mass from all minerals (hornblende, augite, garnet) was within 20% of that from the NIST 612, which demonstrates that the ablation rate with the excimer system was relatively matrix-insensitive. Although fractionation is influenced by the laser wavelength, it is important to remember that many of these studies involve different lasers. In addition to wavelength, these lasers have different properties (pulse duration, coherence, spatial profile, *etc.*).

This manuscript presents a continuing effort to study fractionation effects based on wavelength. In this work, we compare the ablation of NIST glasses and calcite using three wavelengths, 266 nm (fourth harmonic of YAG laser used in many of the commercial systems), 213 nm (the fifth harmonic of the YAG laser) and 157 nm (F_2 excimer laser). The work is the first analytical study using the F_2 excimer laser at 157 nm. The research shows relative effects when the three wavelengths are used for ablation; it is not accurate to compare the excimer and YAG lasers because of different beam properties (pulse duration, spatial profile, coherence, *etc.*). A qualitative comparison of three UV wavelengths is presented, with emphasis on the irradiance and crater development. These studies show that fractionation can be eliminated or enhanced depending on the wavelength and irradiance, and that the choice of laser wavelength should be made on the basis of sample opacity.

Experimental

The experimental system includes three lasers, a PQ3 (VG Elemental) ICP-MS instrument and an ablation cell. The lasers are: a Nd:YAG (New Wave Research) frequency quadrupled

(266 nm) with a 6 ns pulse width, a Nd:YAG (New Wave Research) frequency quintupled (213 nm) with a 6 ns pulse width, and an F_2 excimer (Lambda Physik) with a 30 ns pulse width at 157 nm. A plano-convex lens with a nominal focal length of 20 cm was used with the Nd:YAG lasers. A calcite lens of focal length 15 mm was used for the F_2 excimer laser beam. All lasers were operated at 10 Hz repetition rate. Energy was maintained at 0.8 mJ for all the lasers. Because the 157 nm laser beam does not propagate in air, the F_2 beam path was enclosed in a glove-bag with a continuous Ar gas purge at 2 L min^{-1} .

The laser beam spot diameter was measured by using a single laser pulse with low energy (*ca.* 200 μJ) to cause melting on a single crystal Si sample. Ablation crater diameters were measured from images using a white-light interferometric microscope (New View 200, Zygo Corporation). A depth map of a crater measured using the white-light interferometric microscope on single crystal Si is shown in Fig. 1 to demonstrate the laser beam profile.

A description of the ablation chamber can be found elsewhere.¹⁹ Samples were placed on an XYZ translation stage with manual controls. The ICP-MS signal intensity data were acquired in the time-resolved mode during continuous ablation on a single sample surface, using time-resolved analysis (TRA) software. A dwell time of 24 ms per isotope and single point per peak were used throughout these experiments. Background correction was applied in all cases, before calculating the intensity and intensity ratio. NIST glass reference standards (610, 612, 614) and calcite samples were used in this study. The concentration of these NIST glass standards can be found in refs. 20–22.

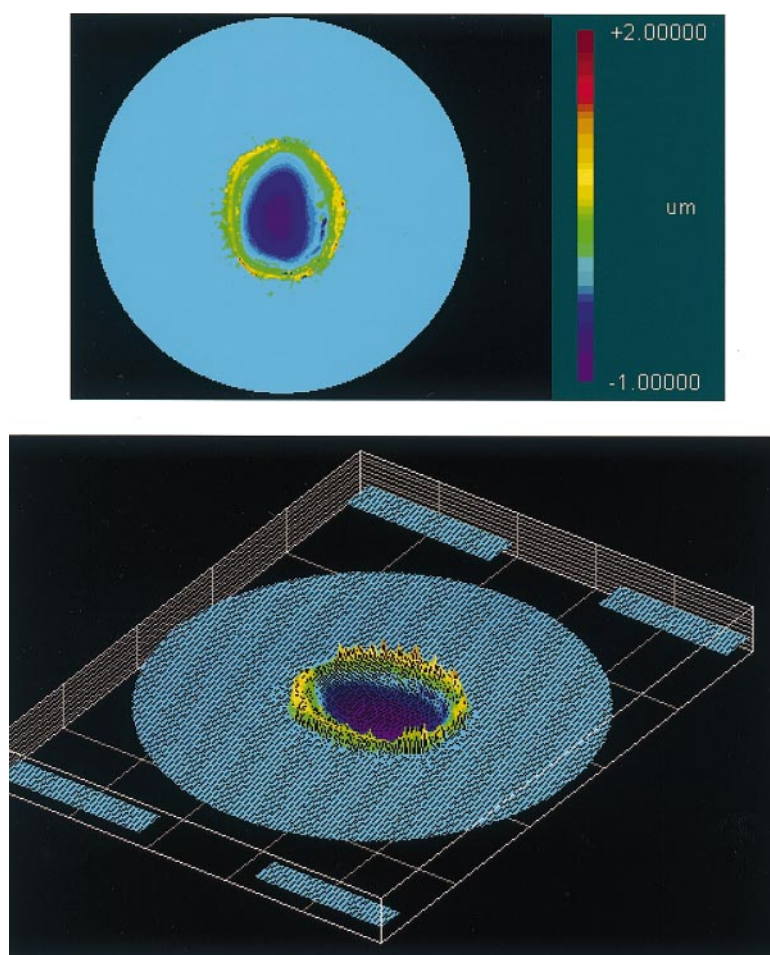


Fig. 1 A depth map of the crater measured by the white-light interferometric microscope on a single crystal Si.

Results and discussion

This research demonstrates that fractionation can be minimized or enhanced at any of the wavelengths studied herein. The temporal behavior of Ca, ablated from three NIST glasses using the 157 nm excimer laser beam, is shown in Fig. 2. Ca has approximately the same nominal concentration in all three standards. Each glass shows similar ICP-MS temporal behavior; the quantity of mass ablated is the same regardless of wavelength and number of pulses. Although optical absorption data for these NIST standards at 157 nm are not available, it is assumed that each standard is 'opaque' at this wavelength. Visually, the glasses go from dark blue (610) to semi-transparent (614). Ablation was at a fluence of 1.3 J cm^{-2} , the highest achieved with this laser based on energy, beam profile and focusing lens. At this fluence, ablation is evident from the first pulse. For successive pulses, the change in signal intensity represents a change in the ablation rate. The normalized (to concentration) Pb to Ca intensity ratios are shown in Fig. 3(a). In general, the ratio and time-dependent data vary with laser fluence. At this fluence (1.3 J cm^{-2}), the Pb/Ca ratio of the visually transparent 614 Glass initially exhibits a higher value compared to the more opaque 610 and 612 standards; the quantity of Ca ablated was similar, but not the quantity of Pb. Because of the low concentration of Pb in 614 Glass ($\approx 2 \text{ ppm}$), a small amount of contamination of Pb on the surface might cause the observed Pb/Ca ratio behavior. An accurate measurement of the Pb/U ratio is important for geochronology. The Pb/U ratio *versus* number of laser pulses is shown in Fig. 3(b). The behavior of the Pb/U ratio is similar to that of the Pb/Ca ratio.

Ca ICP-MS intensities during ablation of NIST 610 Glass using the 266 and 213 nm laser wavelengths are shown in Fig. 4. The fluence is 1.3 J cm^{-2} , the same as used with the excimer laser for data in Figs. 2 and 3. At this fluence, only the NIST 610 Glass could be sufficiently ablated by 266 nm Nd:YAG laser to provide reliable ICP-MS intensity. The 213 nm laser ablation produces a Ca intensity similar to that measured using the 157 nm laser beam (*cf.*, Fig. 2). The change in ablation rate is also similar; the signal decay represents a change in the amount of mass ablated as the crater is formed. For the 266 nm laser, only the first few pulses ablated a significant amount of Ca detected by the ICP-MS. Similar behavior was observed when using 266 nm with fluence just above the ablation threshold for many 'transparent' samples. The surface chemistry or morphology may be responsible for

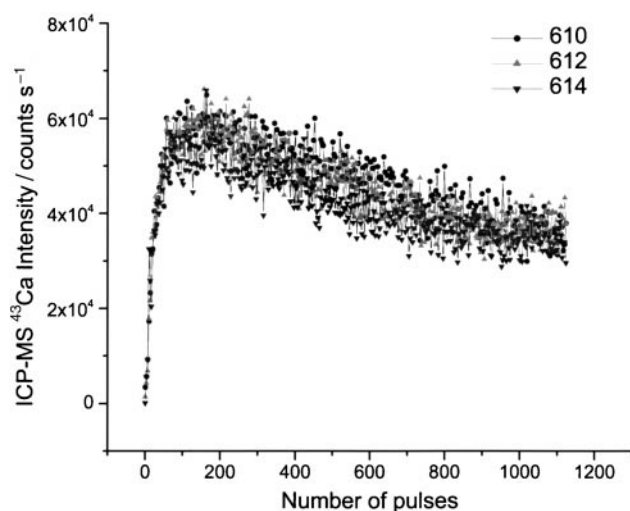


Fig. 2 Ca intensity using F_2 (157 nm) excimer laser at 1.3 J cm^{-2} . The temporal profile (intensity behavior) is almost identical for the NIST 610, 612 and 614 samples. Ca concentration is approximately 12% (as calcium oxide) in all the samples.

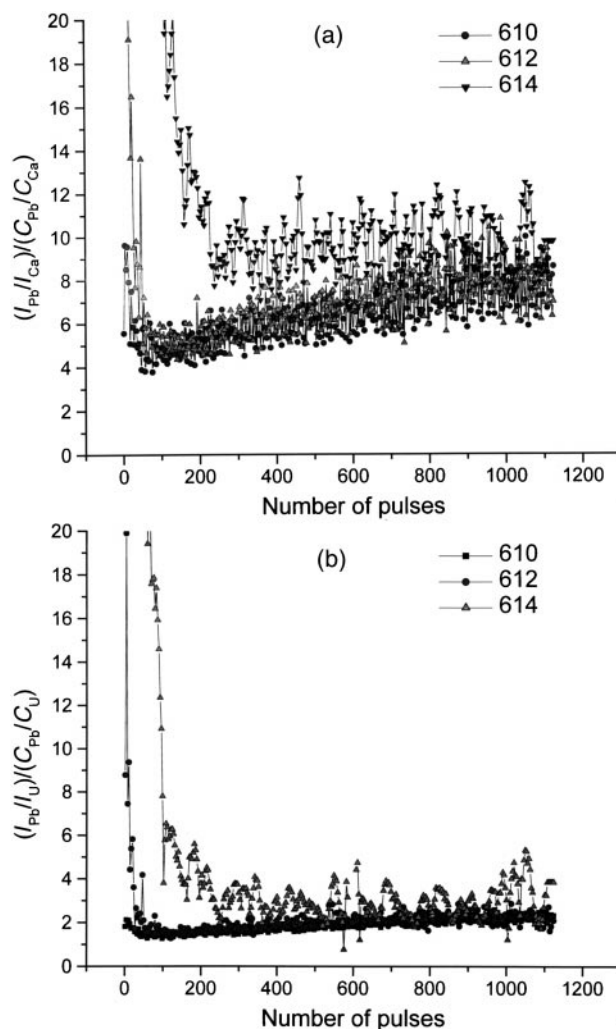


Fig. 3 Normalized Pb/Ca (a) and Pb/U (b) ratios. NIST 614 is more transparent than 610 and 612. Pb concentration ranges from about 400 ppm in NIST 610 compared to about 2 ppm in NIST 614.

the initial ablation behavior as compared with the bulk. The difference in ablation behavior between the 213 nm and 266 nm wavelengths is believed to be due to the optical penetration depth in this NIST Glass; the 213 nm energy will be absorbed in

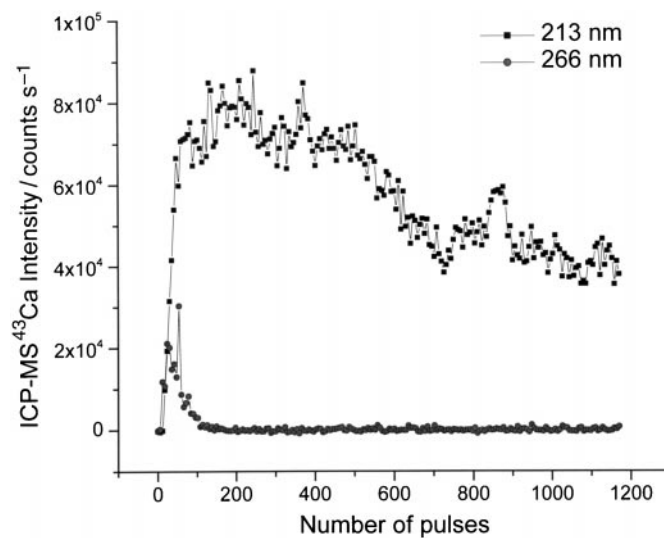


Fig. 4 Ca intensity measured during ablation of NIST 610 using the 213 nm and 266 nm at 1.3 J cm^{-2} . The behaviour of the 213 nm is similar to that measured using 157 nm. The 266 nm does not ablate strongly at this fluence.

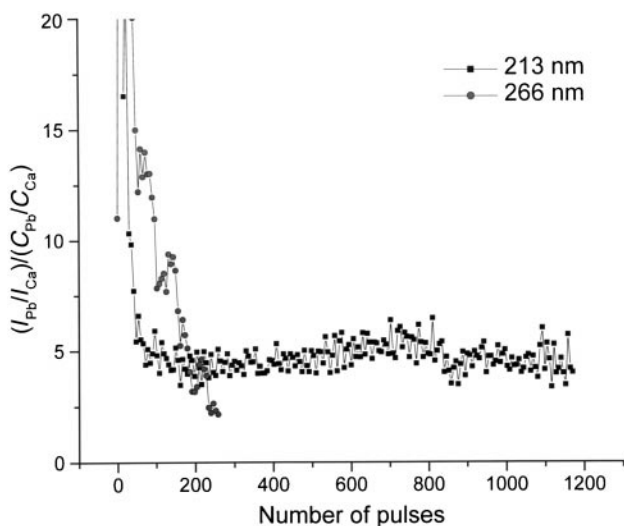


Fig. 5 Normalized Pb/Ca ratio for NIST 610. The ratio measured using 213 nm is similar to that measured using 157 nm. The ratio for 266 nm is not plotted after 200 pulses because of the low signal level at this fluence.

a shorter layer. Therefore, the laser energy per unit volume is greater. The normalized Pb to Ca intensity ratios are shown in Fig. 5. The stabilized ratio at 213 nm is similar to that measured using 157 nm (*cf.*, Fig. 3). For NIST 614 Glass, the ratio behavior is similar to that of NIST 610 but with a larger

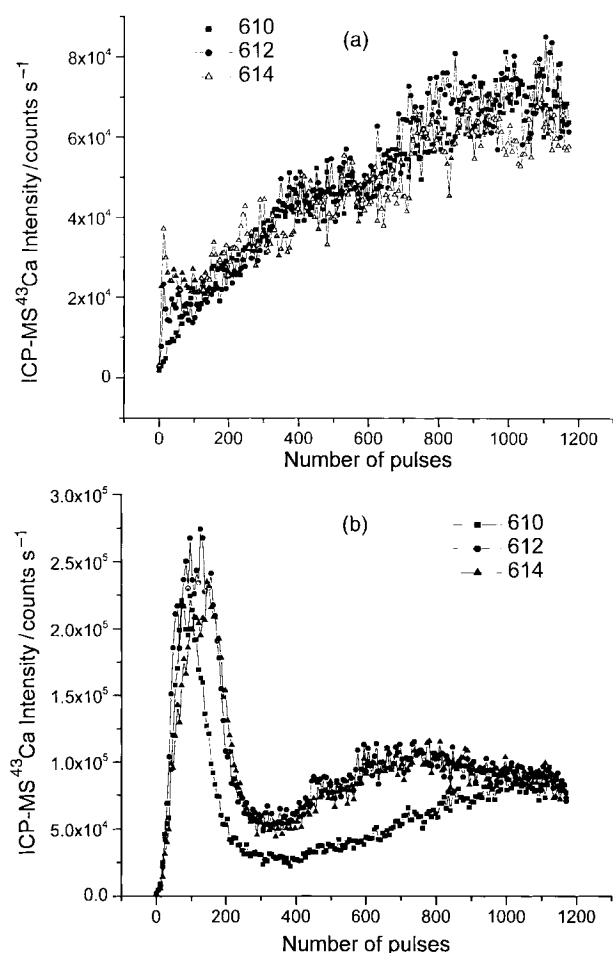


Fig. 6 Temporal profiles of Ca intensity for the three NIST samples using 213 nm (a), and 266 nm (b) at 12 J cm^{-2} . The 213 nm provides a similar intensity profile and does not produce an initial peak for all three NIST samples. The 266 nm does show a difference in signal intensity and the initial peak. The differences are probably caused by optical absorption of the three samples at 266 nm and 213 nm.

error because of the lower concentration of Pb. The ratio obtained with the 266 nm laser after 200 pulses was not plotted because of the low signal intensity. The ratio and its time-dependence depend on the laser-beam fluence and wavelength, and optical properties of the sample.

The above data were measured at a relatively low fluence, a region in which thermal vaporization may be dominant, to demonstrate the influence of wavelength on fractionation. A higher fluence can be utilized to increase the quantity of ablated mass and to reduce fractionation.⁷ Fig. 6 shows the Ca intensity during ablation of the three NIST glasses using 213 nm [Fig. 6(a)] and 266 nm [Fig. 6(b)] at 12 J cm^{-2} . Using 213 nm, each NIST sample exhibits similar ablation behavior (the optical absorption of these glasses was measured to be similar at 213 nm). At this fluence, the amount of mass increases as the crater is formed, in contrast to the low fluence experiments. The ICP-MS intensity is less than that ablated at 1.3 J cm^{-2} initially and then increases gradually. In both cases, the laser energy was approximately 0.8 mJ. The laser beam spot size on the sample defines the fluence. The total ablated mass is proportional to the fluence and the ablated spot area. With a larger spot size (≈ 10 times larger), a lower fluence can provide more ablated mass than for a higher fluence with a small spot size. Using 266 nm, an intense signal is measured initially, much greater than that for the 213 nm wavelength, but it decays quickly. The overall behavior is due to the growth of the crater and its effects on the irradiance and plasma properties. The larger initial signal intensity using 266 nm may be due to

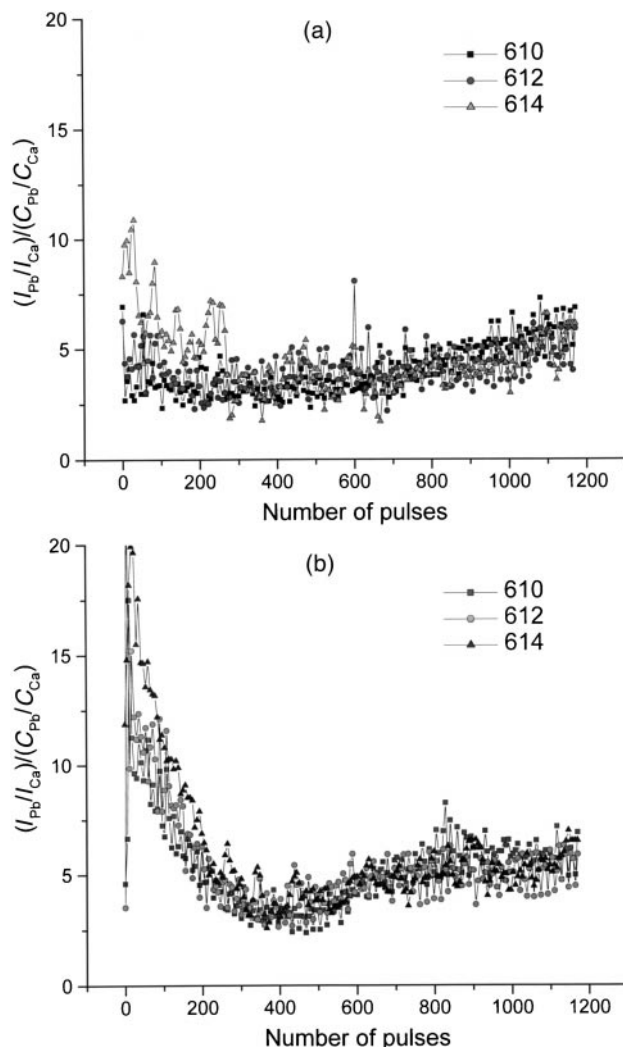


Fig. 7 Normalized Pb/Ca ratios for the three NIST samples using 213 nm (a) and 266 nm (b) at 12 J cm^{-2} .

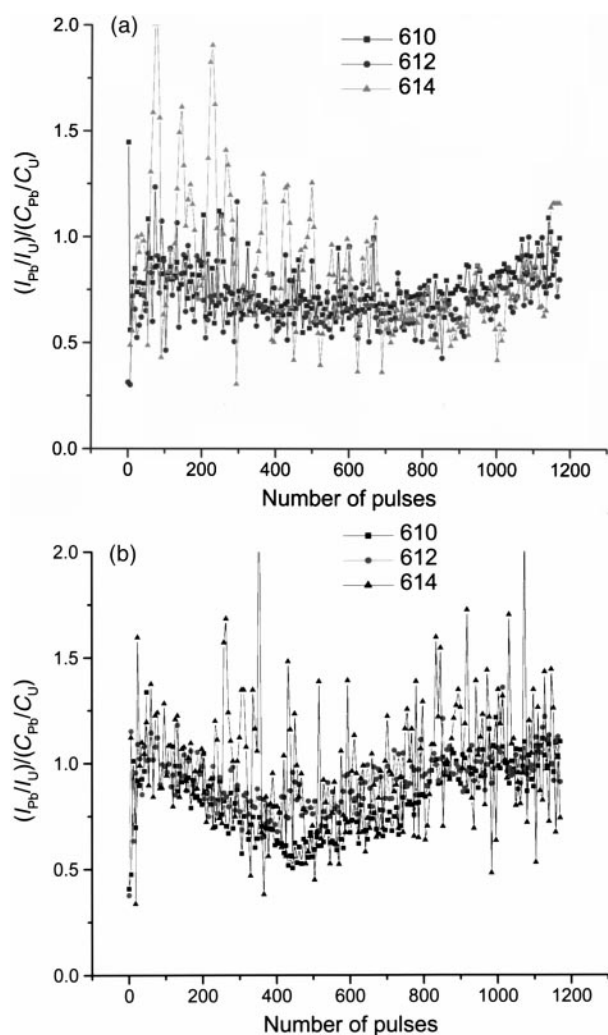


Fig. 8 Normalized Pb/U ratios for the three NIST samples using 213 nm (a) and 266 nm (b) at 12 J cm^{-2} .

the optical penetration depth. Since the irradiance is well above the ablation threshold, a larger volume of mass is ablated for each pulse. In turn, the crater will develop faster, which explains the structured time-dependent behaviour. Fig. 7 shows the normalized Pb to Ca ratios for these glasses using 213 nm [Fig. 7(a)] and 266 nm [Fig. 7(b)] lasers. At this high fluence, the time-dependent fractionation is strongly influenced by the laser wavelength. The optical properties of the samples have a relatively smaller influence on fractionation behavior [compare data within Fig. 7(a) or (b)]. For 266 nm, the initial normalized ratio of Pb/Ca was approximately 12 and dropped to 3 after approximately 400 pulses. The change in the ratio is approximately 4 times. The Pb/U ratios for wavelengths 213 and 266 nm are shown in Fig. 8(a) and (b). The temporal behavior is similar to that of Pb/Ca ratios. For a 266 nm wavelength, the initial normalized ratio is 1.1 and drops to 0.7 after approximately 400 pulses.

The above fluences were selected as test cases to demonstrate how fractionation is influenced by laser-beam wavelength. At any fluence, wavelength influences the quantity of mass ablated per pulse (ablation rate) and elemental fractionation. If the sample is opaque at a particular wavelength, the ablation rate appears to be more reproducible (steady), and a greater quantity of mass is ablated. This effect is demonstrated for the 157 nm laser using calcite as the sample (Fig. 9). Calcite is used as the optical material for lenses and windows for the 157 nm laser. However, at a high fluence, it is relatively easy to ablate calcite. The 157 nm ablation shows similar behavior for calcite as was measured using the NIST glasses. The ICP-MS intensity

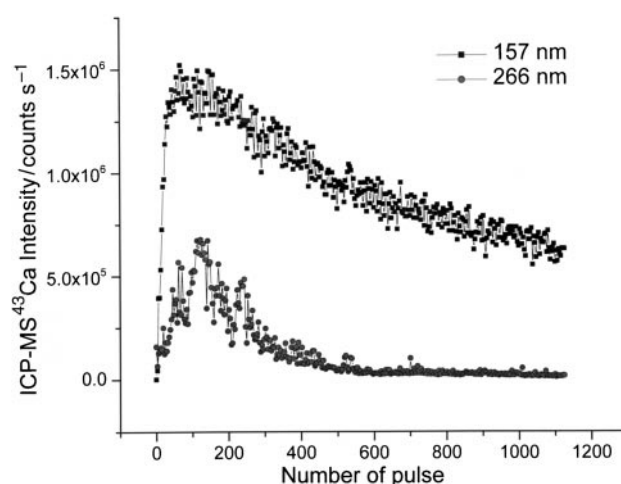


Fig. 9 Ca signal intensity profile for ablation from a calcite sample at 266 nm and 157 nm. Although the fluence was essentially equal, the irradiance was not because of the different pulse width of each laser. At this fluence, 157 nm is more efficient at ablation than the 266 nm laser.

from Ca in calcite is approximately 20 times higher than that from the NIST samples at a similar laser fluence (*cf.*, Fig. 2). The Ca concentration difference in the calcite and NIST samples is only approximately 5 times. The amount of ablated mass strongly depends on the physical properties and the concentration of the sample. The intensity difference between the NIST samples and calcite could be caused by different physical properties of the samples (such as different thermal properties and bonding energy in NIST samples and calcite) and optical penetration depth.

Conclusion

This manuscript demonstrates that wavelength is not the only critical parameter influencing fractionation. Fractionation can be minimized or enhanced in any sample and at any wavelength, depending on the laser-beam irradiance. From our experiences, an irradiance can be established for all wavelengths at which fractionation is not significant or is completely eliminated. Wavelength has a dramatic effect on the quantity of mass ablated and on the ablation rate. The shorter the wavelength, the more controlled or reproducible is the ablation rate. Also, the shorter the wavelength, the lower the fluence that is required to initiate ablation. An increase in signal intensity (quantity of mass ablated and transported to the ICP-MS) directly related to wavelength was not observed. The signal intensity for the 157 nm ablation was similar to that for 213 nm using NIST 610 Glass. It could be that the optical penetration is essentially at the surface for both wavelengths. This is not the case when the sample is transparent; once the fluence is greater than the ablation threshold, the longer wavelength provides greater signal intensity because more mass is ablated from a larger volume. With a larger amount of mass ablated per pulse, the crater deepens faster, effectively reducing the irradiance and trapping the plasma. These effects can lead to enhanced fractionation.

Acknowledgements

The authors acknowledge the technical support and loan of lasers from New Wave Research, Merchantek (213 nm Nd:YAG) and Lambda Physik (157 nm ArF excimer). This research was supported by the Environmental Waste Management Science Program, funded jointly by the Assistant Secretary for Environmental Management and by the Director, Office of Energy Research, of the U.S. Department of Energy, under Contract No. DE-AC03-76SF00098.

References

- 1 R. E. Russo, X. L. Mao, O. V. Borisov and H. C. Liu, in *Encyclopedia of Analytical Chemistry: Instrumentation and Applications*, John Wiley & Sons, New York, 2000.
- 2 S. F. Durrant, *J. Anal. At. Spectrom.*, 1999, **14**, 1385.
- 3 D. Günther, S. E. Jackson and H. P. Longerich, *Spectrochim. Acta, Part B*, 1999, **54B**, 381.
- 4 R. E. Russo, X. L. Mao and O. V. Borisov, *Trends Anal. Chem.*, 1998, **17**, 461.
- 5 P. J. Sylvester and M. Ghaderi, *Chem. Geol.*, 1997, **141**, 49.
- 6 M. L. Alexander, M. R. Smith, I. S. Harman, A. Medoza and D. W. Koppenaal, *Appl. Surf. Sci.*, 1998, **127–129**, 255.
- 7 H. C. Liu, O. V. Borisov, X. L. Mao, S. Shuttleworth and R. E. Russo, *Appl. Spectrosc.*, 2000, **54** (11).
- 8 T. E. Jeffries, N. J. G. Pearce, W. T. Perkins and A. Raith, *Anal. Commun.*, 1996, **33**, 35.
- 9 P. M. Outridge, W. Doherty and D. C. Gregoire, *Spectrochim. Acta, Part B*, 1996, **51B**, 1451.
- 10 P. M. Outridge, W. Doherty and D. C. Gregoire, *Spectrochim. Acta, Part B*, 1997, **52B**, 2093.
- 11 H. P. Longerich, D. Günther and S. E. Jackson, *Fresenius' J. Anal. Chem.*, 1996, **355**, 538.
- 12 T. E. Jeffries, S. E. Jackson and H. P. Longerich, *J. Anal. At. Spectrom.*, 1998, **13**, 935.
- 13 D. Figg and M. S. Kahr, *Appl. Spectrosc.*, 1997, **51**, 1185.
- 14 Z. X. Chen, *J. Anal. At. Spectrom.*, 1999, **14**, 1823.
- 15 A. J. G. Mank and P. R. D. Mason, *J. Anal. At. Spectrom.*, 1999, **14**, 1143.
- 16 D. Günther and C. A. Heinrich, *J. Anal. At. Spectrom.*, 1999, **14**, 1369.
- 17 S. M. Eggins, L. P. J. Kinsley and J. M. G. Shelley, *Appl. Surf. Sci.*, 1998, **127–129**, 278.
- 18 D. Günther, R. Frischknecht, C. A. Heinrich and H. J. Kahlert, *J. Anal. At. Spectrom.*, 1997, **12**, 939.
- 19 A. P. K. Leung, W. T. Chan, X. L. Mao and R. E. Russo, *Anal. Chem.*, 1998, **70**, 4709.
- 20 I. Horn, R. W. Hinton, S. E. Jackson and H. P. Longerich, *Geostand. Newsl.*, 1997, **21**, 191.
- 21 N. J. G. Pearce, W. T. Perkins, J. A. Westgate, M. P. Gorton, S. E. Jackson, C. R. Neal and S. P. Chenery, *Geostand. Newsl.*, 1997, **21**, 115.
- 22 K. Hollocher and J. Ruiz, *Geostand. Newsl.*, 1995, **19**, 27.